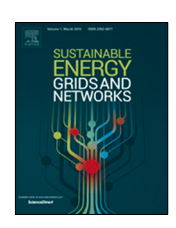
ELSEVIER

Contents lists available at ScienceDirect

Sustainable Energy, Grids and Networks

journal homepage: www.elsevier.com/locate/segan



A graph theory and coalitional game theory-based pre-positioning of movable energy resources for enhanced distribution system resilience



Mukesh Gautam*, Mohammed Benidris

Department of Electrical & Biomedical Engineering, University of Nevada, Reno, Reno, NV, 89557, United States of America

ARTICLE INFO

Article history:
Received 30 September 2022
Received in revised form 15 March 2023
Accepted 29 May 2023
Available online 12 June 2023

Keywords:
Coalitional game
Movable energy resources
Network reconfiguration
Resilience
Spanning forest

ABSTRACT

This article proposes an approach based on graph theory and coalitional game theory for prepositioning of movable energy resources (MERs) to improve the resilience of the electric power supply. By utilizing the weather forecasting and monitoring data, the proposed approach determines staggering locations of MERs in order to ensure the quickest possible response following an extreme event. The proposed approach starts by generating multiple line outage scenarios based on fragility curves of distribution lines, where the fuzzy k-means method is used to create a set of reduced line outage scenarios. The distribution network is modeled as a graph and distribution network reconfiguration is performed for each reduced line outage scenario. The expected load curtailment (ELC) corresponding to each location is calculated using the amount of curtailed load and probability of each reduced scenario. The optimal route to reach each location and its distance is determined using Dijkstra's shortest path algorithm. The MER deployment cost function associated to each location is determined based on the ELC and the optimal distance. The MER deployment cost functions are used to determine candidate locations for MER pre-positioning. Finally, the Shapley value, a solution concept of coalitional game theory, is used to determine the sizes of MERs at each candidate location. The proposed approach for pre-positioning of MERs is validated through case studies performed on a 33-node and a modified IEEE 123-node distribution test systems.

© 2023 Elsevier Ltd. All rights reserved.

1. Introduction

Over the last decade, the frequency of extreme events, both natural (e.g., hurricanes, wildfires, ice or hail storms, and earthquakes) and man-made (e.g., cyber and physical attacks), has increased dramatically. For example, there were 20 weather related catastrophic events in the United States in 2021 alone, each with costs surpassing \$1 billion [1]. Such extreme events have resulted in severe damages to important power system equipment resulting in system-wide extended power outages. The electric companies' goal of delivering reliable and resilient electrical supply to its customers has been compromised by catastrophic weather events and subsequent outages. As a result, effective power distribution service restoration (PDSR) procedures must be established in order to reduce the impact of these incidents on end-user customers. PDSR's major goal is to reduce load curtailments and outage duration by making the best use of available resources. Smart grid technologies, such as microgrid formation, network reconfiguration, repair crew dispatch, distributed generation, energy storage, MERs, and combinations of these

methods and techniques, have proven to be the most effective PDSR solutions.

MERs are mobile and versatile resources that can be redeployed quickly from staggering locations to power outage locations. They are versatile in the notion that they can be built to variable size and quickly integrated into the distribution grid after a disaster. These resources can be designed to supply up to a few megawatts of load. When part of a distribution system is islanded due to equipment failures or damages, MERs can be deployed to supply local and isolated critical loads if no other resources are available [2].

Deployment of MERs for PDSR has gained significant momentum. A two-stage robust optimization framework has been developed in [3] for routing and scheduling MERs to enhance the resilience of distribution systems. A two-stage PDSR strategy based on mixed-integer linear programming (MILP) has been proposed in [4] to enhance seismic resilience of distribution systems with MERs. A mixed integer linear programming-based PDSR strategy has been proposed in [5] for an active distribution system, where routing and scheduling of mobile energy storage systems is performed for enhanced resilience. In [6], a two-stage optimization strategy has been proposed to enhance distribution system resilience with mobile energy storage units, where dynamic microgrid formation is also considered. In [7], the

^{*} Corresponding author.

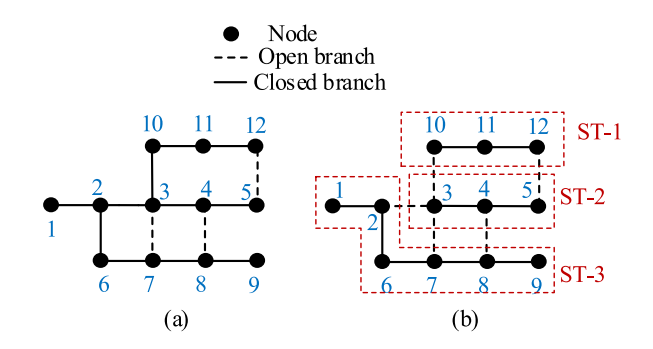
E-mail addresses: mukesh.gautam@nevada.unr.edu (M. Gautam),
mbenidris@unr.edu (M. Benidris).

	Nomenclature	
	\mathcal{N}	Set of players of a coalitional game
	V	Characteristic function
	S	Coalition that is subset of $\mathcal N$
	$2^{\mathcal{N}}$	Possible set of coalitions
	ELC_i	Expected load curtailment of location i
	CDF_i	Capacity distribution factor of location i
	ψ_i	Shapley value of player i
	r	Number of original scenarios
	K	Number of reduced scenarios
	Pr(j)	Probability of the j^{th} reduced scenario
	β_1,β_2	Cost function weighting coefficients
	ω_{m}	Critical load factor at node m
	$P_{MER-tot}$	Total MER capacity
	PDSR	Power distribution service restoration
	MER	Movable energy resource
	ECLR	Expected critical load recovery
ı		

scheduling of mobile energy storage systems has been performed by formulating a stochastic optimization problem. A two-stage robust optimization problem has been proposed in [8] for the optimal dispatch of mobile power sources for minimization of critical load curtailment. The majority of the aforementioned studies primarily focus on coordinating and dispatching MERs with other PDSR techniques for service restoration, without considering MER pre-positioning.

This article proposes an approach based on graph theory and coalitional game theory for pre-positioning of MERs. High wind speed caused by hurricanes or tornadoes is taken as an example of weather-related extreme events. A set of line outage scenarios is generated based on forecasted wind speed. Generated scenarios are then reduced using the fuzzy k-means method. The reduced scenarios are used to determine expected load curtailments when MERs are placed at each node. The MER deployment cost function of each node is determined using expected load curtailment and the optimal distance of MER deployment location calculated using Dijkstra's shortest path algorithm. A certain number of candidate locations of MERs is selected based on the MER deployment cost function. The candidate locations thus selected are treated as players of a game. Since the players are allowed to form coalitions among themselves to maximize the expected critical load recovery, the game is a coalitional game. Shapley value, one of the solution concepts of coalitional game theory, is then used to determine sizes of MERs at each candidate location. The proposed approach is validated through case studies on several distribution test systems. The main contributions of this article include developing:

- A framework for pre-positioning of MERs as a proactive measure for enhanced distribution system resilience.
- A graph theoretic approach to determine the total amount
 of curtailed critical loads. The graph theory is used to create
 microgrids energized with MERs and the critical load curtailments of all microgrids and isolated parts of the distribution
 network are added to find the total critical load curtailment.
- A MER deployment cost function calculated for each location based on the weighted combination of the expected load curtailment and the optimal distance. The MER deployment cost function serves a criterion to determine candidate locations for MER deployment.
- A coalitional game theoretic framework find the individual sizes of MERs at each candidate location. The coalitional



 ${f Fig.~1.}$ (a) A spanning tree; and (b) a spanning forest of a hypothetical 12-node system.

game theoretic approaches have the ability to uniquely assign payoffs among players of the game.

The remainder of the article is organized as follows. The mathematical modeling of the MER pre-positioning problem is explained in Section 2. The proposed approach and solution algorithm are described in Section 3. Case studies on two different distribution test systems are used to validate the proposed work in Section 4. Section 5 provides some concluding remarks and future research directions.

2. Mathematical modeling

This section presents the graph theoretic modeling of distribution network and road network, and the coalitional game theoretic model of the MER pre-positioning problem under study for resilience enhancement of the distribution system.

2.1. Graph theoretic modeling of distribution network

Distribution systems are equipped with sectionalizing switches (normally closed) and tie-switches (normally open). When all the switches of a distribution network are closed, a meshed network is formed, and the meshed network thus formed can be represented by an undirected graph $\mathcal{G} = (\mathbb{N}, \mathcal{E})$, where \mathbb{N} is a set of nodes (or vertices) and \mathcal{E} is a set of edges (or branches).

2.1.1. Spanning tree

A spanning tree is defined as a subset of the undirected graph $\mathcal{G}=(\mathbb{N},\mathcal{E})$ that has a minimal number of edges linking all vertices (or nodes). In a spanning tree, the number of edges is one less than the number of vertices. There are no cycles in a spanning tree, and all of the vertices are connected [9]. A linked graph can have many spanning trees, each of which has the same number of edges and vertices. Each of the undirected graph \mathcal{G} 's edges has a specific value (or weights). The edge weights vary depending on the problem. The sum of all edge weights of a spanning tree is minimized when establishing the minimum spanning tree. Fig. 1(a) shows a spanning tree of a hypothetical 12-node system. The spanning tree shown in the figure consists of all system nodes (i.e., 12) and 11 closed branches (edges).

2.1.2. Spanning forest

In graph theory, a forest is a disconnected union of trees. A spanning forest is a forest that covers all vertices of the undirected graph \mathcal{G} and consists of a set of disconnected spanning trees [9]. When all spanning trees are connected, each vertex of the undirected graph \mathcal{G} is included in one of the spanning trees [10]. On the other hand, when a disconnected graph has many connected components, a spanning forest is formed and

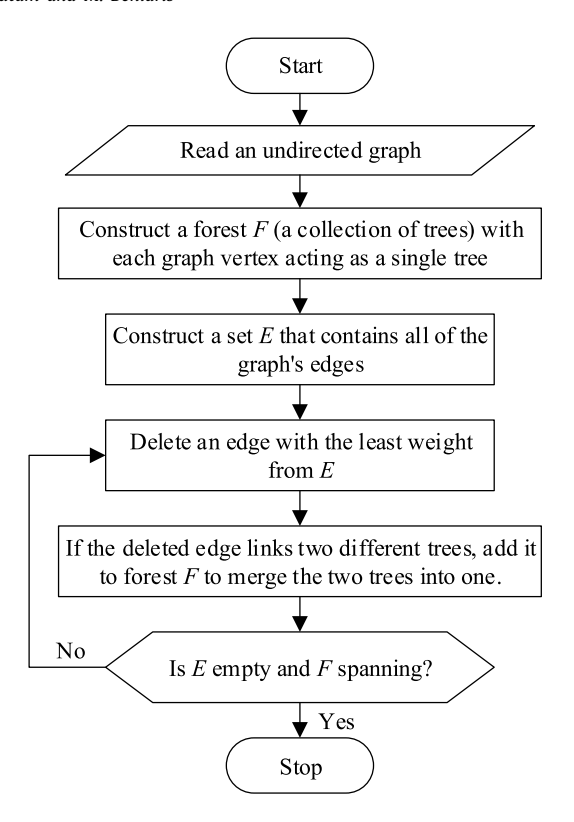


Fig. 2. Flowchart of Kruskal's spanning forest search algorithm.

it contains a spanning tree of each component [11]. Fig. 1(b) shows the spanning forest formed as a result of disconnection of two additional branches (2–3 and 3–10) in the spanning tree presented in Fig. 1(a). The spanning forest shown in Fig. 1(b) consists of three spanning trees (ST-1, ST-2, and ST-3).

In this article, Kruskal's algorithm [12] is used to search for the optimal spanning forest. Kruskal's spanning forest search algorithm (KSFSA) starts by constructing a forest F with each graph vertex acting as a single tree based on the given undirected graph. Since KSFSA is a greedy algorithm, it goes on connecting the next least-weight edge that avoids loop or cycle to the forest F at each iteration. The resulting forest F after the last iteration is the optimal spanning forest. Fig. 2 shows the flowchart of KSFSA.

2.2. Graph theoretic modeling of road network—Dijkstra's shortest path algorithm

A road network refers to a collection of linked points and lines that depict a network of roads in a certain area. The road network may be modeled using the graph theory since it consists of linked points and lines that resemble vertices and edges in a graph. In this article, the meshed configuration of the road network is modeled as an undirected graph $\mathcal{G}_r = (\mathcal{N}_r, \mathcal{E}_r)$, where \mathcal{N}_r is a set of nodes and \mathcal{E}_r is a set of road edges. The weight of each road edge is determined by its length.

Since multiple routes from the initial location of MERs to the final location may be possible, determining the best route can significantly minimize the MER deployment cost function. In this work, Dijkstra's Shortest Path Algorithm (DSPA) is used to find the shortest (optimal) path between two different nodes of a road network graph. DSPA uses the least edge weight to calculate the shortest path from the initial location to the destination. DSPA can only be applied in case of the graph with non-negative edge weights [13]. DSPA is appropriate for this study since the length of

each road edge (which is non-negative) is used to calculate edge weights.

2.3. Coalitional game theory and shapley value

In game theory, coalitional game refers to the game where players can establish alliances or coalitions with one another to maximize coalitional and individual utilities. Since coalitions among players are formed to increase their individual incentives, a coalition must always result in equal or greater incentives than individual player's incentives [14]. A coalitional game is defined by assigning a value to each of the coalitions. The coalitional game is composed of the following two components:

- ullet A finite players' set \mathcal{N} , known as the grand coalition.
- A characteristic function $V(S): 2^{\mathcal{N}} \to \mathbb{R}$ that maps the set of all possible player coalitions to a set of coalitional values that satisfy $V(\phi) = 0$.

The characteristic function, representing the worth or value of each coalition, is defined in every coalitional game. The characteristic function of a coalition is the aggregated worth of all coalition members. Solution paradigms such as the Shapley value, the core, the Nucleolus, and the Nash-bargaining solution are used to allocate the overall payout or incentive among individual players of a coalitional game.

2.3.1. The core of a coalitional game

In game theory, the core is the set of possible assignments that cannot be enhanced more through any alternative coalitions. The core is a set of payout assignments that ensures no player or player group has a motivation to quit $\mathcal N$ to establish a new coalition. Mathematically, the core is defined as follows [15].

$$C = \left\{ \alpha : \sum_{j \in \mathcal{N}} \alpha_j = V(\mathcal{N}) \text{ and } \sum_{j \in S} \alpha_j \ge V(S), \forall S \subset \mathcal{N} \right\}$$
 (1)

2.3.2. The shapley value

The Shapley value is a solution paradigm of coalitional game theory. The Shapley value is an approach to allocate the overall earnings to individual players when all participants participate in the game. The Shapley value of a coalitional game is expressed as follows [16].

$$\psi_{j}(V) = \sum_{S \in 2^{\mathcal{N}}, j \in S} \frac{(|S| - 1)!(n - |S|)!}{n!} [V(S) - V(S \setminus \{j\})]$$
 (2)

where $n = |\mathcal{N}|$ is the total number of players.

The Shapley value has a number of important properties, which are listed below:

• Efficiency: The efficiency property is stated as follows.

$$\sum_{j\in\mathcal{N}} \psi_j(V) = V(\mathcal{N}) \tag{3}$$

 Individual Rationality: The individual rationality property is stated as follows.

$$\psi_i(V) \ge V(\{j\}), \forall j \in \mathcal{N}$$
 (4)

• *Symmetricity:* For two players i and j satisfying $V(S \cup \{i\}) = V(S \cup \{j\})$ for each coalition S without i and j,

$$\psi_i(V) = \psi_i(V) \tag{5}$$

• *Dumminess*: For player i satisfying $V(S) = V(S \cup \{i\})$ for each coalition S without i,

$$\psi_i(V) = 0 \tag{6}$$

• *Linearity:* For two characteristic functions V_1 and V_2 of a coalitional game,

$$\psi(V_1 + V_2) = \psi(V_1) + \psi(V_2) \tag{7}$$

3. Pre-positioning of MERs

This section presents event modeling, scenario generation and reduction, and formulation of the coalitional game.

3.1. Extreme event modeling and scenario generation

In this work, the weather-related fragility curve is used to model the impacts of extreme events on system and generate multiple line outage scenarios. A fragility curve is applied to characterize the performance and vulnerabilities of different system components confronting uncertain weather-related extreme events. The failure probabilities of each component are obtained by mapping the weather forecast and monitoring data to the fragility curve [17]. We have taken the multiple line outages caused by high wind speeds as an example of a weather-related extreme event in this study. Mathematically, the probability of line outages caused by high wind speeds can be represented as follows [18].

$$P_{l}(w) = \begin{cases} \overline{P_{l}}, & \text{if } w < w_{\text{crl}} \\ P_{l \perp hw}(w), & \text{if } w_{\text{crl}} \le w < w_{\text{cpse}} \\ 1, & \text{if } w \ge w_{\text{cpse}} \end{cases}$$
 (8)

where P_l is the probability of line failure as a function of wind speed w; $\overline{P_l}$ is the failure probability at normal weather condition; $P_{l,hw}$ is the probability of line failure at high wind; w_{crl} is the critical wind speed (i.e., the speed above which the distribution lines start experiencing failure); and w_{cpse} is the speed above which the distribution lines completely collapse.

3.2. Scenario reduction using Fuzzy k-means method

The accuracy of an approach is always improved when a large number of line outage scenarios is used. However, solving the problem with a large number of scenarios takes a long time. The generated line outage scenarios are, therefore, reduced using the fuzzy k-means method in this work to make the proposed approach computationally tractable. The fuzzy k-means clustering, also referred to as soft clustering, is a type of clustering or scenario reduction in which each scenario can be a member of multiple reduced scenarios. There is fuzziness or overlap between different clusters in case of the fuzzy k-means method.

Consider an original set of scenarios $\mathcal{X} = \{x_1, \dots, x_r\}$ and $\mathcal{M} = \{\mu_1, \dots, \mu_K\}$ be the set of reduced scenarios (cluster centroids). If the degree of membership of any data point x_i from \mathcal{X} with the jth cluster of scenarios is defined by a weight u_{ji} , then the cluster centroid of the jth reduced scenario is obtained by taking the weighted mean of all original scenarios, mathematically expressed as follows.

$$\mu_{j} = \frac{\sum_{i=1}^{r} u_{ji}^{m} \times x_{i}}{\sum_{i=1}^{r} u_{ii}^{m}},$$
(9)

where m is the hyperparameter that determines fuzziness of the clusters.

To obtain the final values of cluster centroids, the objective function (10) is iteratively minimized [19].

$$\min \sum_{i=1}^{r} \sum_{i=1}^{K} u_{ji}^{m} \|x_{i} - \mu_{j}\|^{2}, \tag{10}$$

where

$$u_{ji} = \frac{1}{\sum_{k=1}^{K} {\binom{\|x_i - \mu_j\|}{\|x_i - \mu_k\|}}^{\frac{2}{m-1}}}$$
(11)

In order to evaluate the effectiveness of scenario reduction, the fuzzy k-means method is compared with k-means and k-medians methods in terms of Silhouette (SL) index, Davies-Bouldin (DB) index, and Calinski-Harabasz (CH) index.

The SL index evaluates an original scenario's cohesiveness with its own cluster in comparison to other clusters. The range of SL index is from 1 to +1, and a larger value implies a good fit to the scenario's own cluster and a poor fit to other clusters. The SL index is mathematically defined as follows [20].

$$S_{L} = \frac{1}{r} \sum_{i=1}^{r} \left(\frac{b_{i} - a_{i}}{\max\{a_{i}, b_{i}\}} \right), \tag{12}$$

where a_i denotes the average distance between the *i*th scenario and other scenarios in the same cluster (i.e., cohesiveness) and b_i denotes the minimum distance between the *i*th scenario and other scenarios of other clusters (i.e., separation).

The DB index utilizes the intrinsic properties and features of dataset to validate the effectiveness of the clustering. The DB index compares each cluster's mean similarity to that of its closest neighbor, where similarity is defined as the ratio of intra-cluster to between inter-cluster distances [21]. Therefore, clusters that are more evenly spaced apart will be assigned higher score. With a minimum value of 0, better clustering is indicated by lower numbers. Mathematically, the DB index is defined as follows [21].

$$DB = \frac{1}{K} \sum_{j=1}^{K} \max_{i \neq j} \frac{S_j + S_i}{M_{ji}},$$
(13)

where S_j is a measure of intra-cluster distance of the jth cluster and M_{ji} is a measure of inter-cluster distance between clusters j and i.

The CH index is an index that evaluates the degree of dispersion between different clusters. The CH index refers to the ratio of inter-cluster dispersion to intra-cluster dispersion [22]. It is also referred to as the variance ratio index. The larger value of CH index indicates better clustering. Mathematically, the CH index is expressed as follows [22].

$$CH = \frac{B_K \times (r - K)}{W_K \times (K - 1)},\tag{14}$$

where B_K denotes inter-cluster covariance and W_K denotes intracluster covariance.

3.3. Selection of candidate MER locations

For the selection of candidate MER locations, the MER deployment cost function is used, which is calculated based on the expected load curtailment (ELC) of each location and the optimal distance of MER deployment location from the initial MER location. The ELC corresponding to the *i*th location is determined using the amount of curtailed critical load for each reduced line outage scenario as follows.

$$ELC_{i} = \sum_{i=1}^{K} Pr(j) \times LC_{i}(j), \tag{15}$$

where K is the total number of reduced scenarios; Pr(j) is the probability of the jth reduced scenario; and $LC_i(j)$ is the critical

load curtailment of the *j*th reduced scenario for MER deployment location *i*, which is calculated as follows.

$$LC_i(j) = \sum_{m=1}^{N} \omega_m \Delta P_{mi}(j), \tag{16}$$

where $\Delta P_{mi}(j)$ is the load curtailment at node m of the jth reduced scenario for MER deployment location i; ω_m is the critical load factor at node m; and N is the total number of nodes in the system.

While computing the critical load curtailment, the nodal power balance constraints and radiality constraint should always be satisfied, which are described below.

(a) Node power balance constraints: The power balance constraint at each node of the system can be expressed as follows.

$$\sum_{r \in \Omega_{g}(r)} P_{g,r} + \sum_{l \in \Omega_{L}(r)} P_{l,r} = P_{D,r}$$

$$\tag{17}$$

where $\Omega_g(r)$ is the set of sources (including MER) connected to node r; $\Omega_L(r)$ is the set of lines connected to node r; $P_{g,r}$ is the power injected from source r; $P_{D,r}$ is the load at node r; and $P_{l,r}$ is the line power flow from node l to node r.

(b) Radiality constraint: A distribution system must always meet the radiality requirement. Therefore, each potential configuration should be radial (i.e., the radiality constraint should be met for each spanning tree of the network). Each spanning tree of the network is represented by a sub-graph $\mathcal{G}_s = (\mathcal{N}_s, \mathcal{E}_s)$, where \mathcal{N}_s is a set of nodes (or vertices) and \mathcal{E}_s is a set of edges (or branches) in the sub-graph. For the sub-graph, a node-branch incidence matrix should be constructed. If $n_s = |\mathcal{N}_s|$ denotes the number of nodes and $e_s = |\mathcal{E}_s|$ denotes the number of edges of a particular spanning tree, then the node-branch incidence matrix $A \in \mathbb{R}^{n_s \times e_s}$ is the matrix with element a_{ij} calculated based on (18). If the node-branch incidence matrix A is full ranked, then the radiality constraint is satisfied.

$$a_{ij} = \begin{cases} +1 & \text{if branch } j \text{ starts at node } i \\ -1 & \text{if branch } j \text{ ends at node } i \\ 0 & \text{otherwise} \end{cases}$$
 (18)

The second component of the MER deployment cost function is the optimal distance of MER deployment location from the initial MER location, which is determined using the DSPA. The MER deployment cost function of the *i*th location is expressed as follows.

$$C_i = \beta_1 \times ELC_i + \beta_2 \times d_i, \tag{19}$$

where ELC_i is the expected load curtailment corresponding to the ith location; d_i is the optimal distance of MER deployment location i from the initial MER location; and β_1 and β_2 are weighting coefficients which sum to unity.

A certain number of candidate MER locations is selected based on least MER deployment cost functions. Determination of the optimum number of candidate MER locations is beyond the scope of this work; readers are referred to our previous work [23] for the determination of the optimal number of MERs.

3.4. Computation of characteristic functions of the coalitional game model

A coalitional game model is formulated considering candidate MER locations as players of the game. The list of all possible coalitions of candidate MER locations is generated. For example, if three candidate MER locations (L_1 , L_2 , and L_3) are selected, the set of all possible coalitions, denoted by $2^{\mathcal{N}}$, is as follows.

$$2^{\mathcal{N}} = \{\phi, \{L_1\}, \{L_2\}, \{L_3\}, \{L_1, L_2\}, \{L_1, L_3\}, \{L_2, L_3\}, \{L_1, L_2, L_3\}\},\$$

where ϕ denotes an empty set.

For each set of coalitions, the expected critical load recovery (ECLR) is computed by taking the difference of ELCs before and after MER placement. The ECLR serves as the characteristic function of each coalition.

3.5. Determination of MER sizes at candidate locations

After computation of characteristic functions of all possible sets of coalitions, Shapley values of each candidate MER location are determined using (2). Based on the Shapley values, the capacity distribution factor (CDF) of the candidate MER location, *i*, is determined as follows.

$$CDF_i = \frac{\psi_i}{\sum_{k=1}^n \psi_k},\tag{20}$$

where ψ_i is the Shapley value of the *i*th location; and n is the number of candidate MER locations.

Now, the total size of MERs is distributed among different candidate MER locations based on CDF as follows.

$$P_{MER-i} = CDF_i \times P_{MER-tot} \tag{21}$$

where P_{MER-i} is the size of MER at the *i*th candidate location; and $P_{MER-tot}$ is the total MER capacity.

3.6. Overall framework and proposed solution algorithm

The overall framework of the proposed approach for prepositioning of MERs is shown in Fig. 3. As shown in the figure, weather forecasting and monitoring data, optimal number of MERs, and optimal total size of MERs are taken as inputs. The proposed approach consists of various modules including ELC calculation module, coalition module, ECLR module, Shapley value module, and capacity distribution module. The outputs of the proposed approach are pre-positioning location of MERs and individual sizes of MERs.

The proposed approach or the solution algorithm for prepositioning of MERs can be summarized as follows.

- 1. Collect system data including generation data, line data, load data, etc., which serve as input to the proposed model.
- 2. Generate a set of line outage scenarios based on weather forecasting and monitoring data.
- 3. Generate a set of reduced scenarios along with their probabilities using a scenario reduction technique.
- Determine expected load curtailments corresponding to each location after MER placement.
- 5. Select a certain number of candidate MER locations based on expected load curtailments.
- 6. Generate the list of all possible coalitions of candidate MER locations using coalition module. For example, if three candidate MER locations (L_1 , L_2 , and L_3) are selected, the set of all possible coalitions, denoted by 2^N , is as follows.

$$2^{\mathcal{N}} = \{\phi, \{L_1\}, \{L_2\}, \{L_3\}, \{L_1, L_2\}, \{L_1, L_3\}, \{L_2, L_3\}, \{L_1, L_2, L_3\}\},\$$

where ϕ denotes an empty set.

- 7. For each set of coalitions, compute expected load curtailments before and after MER placement and compute the difference which serves as the characteristic function.
- 8. After the evaluation of all possible sets of coalitions, compute Shapley value of each candidate MER location using (2).
- 9. Based on the Shapley values, compute the capacity distribution factor (CDF) of each candidate MER location and determine the sizes of each MER.

The flowchart of the proposed approach for pre-positioning of MERs is shown in Fig. 4.

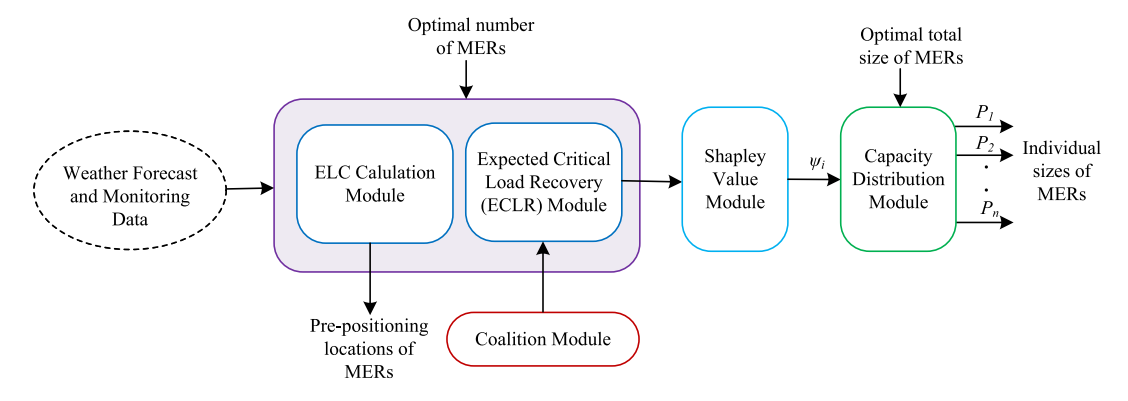


Fig. 3. Overall framework of the proposed approach.

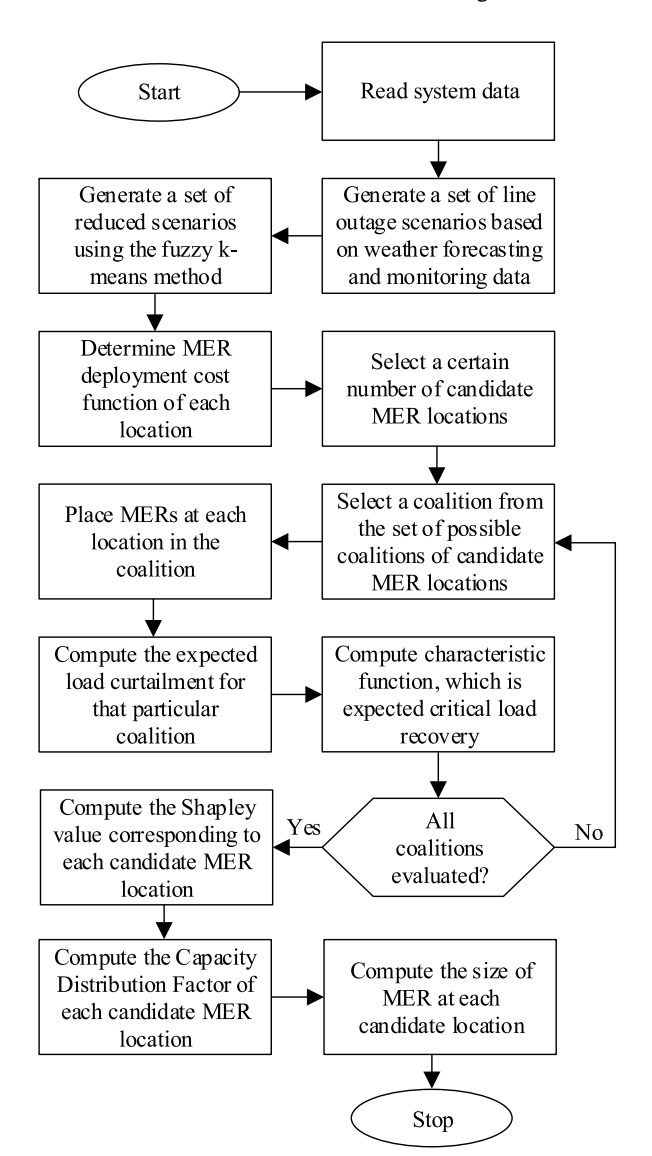


Fig. 4. Flowchart of the proposed approach for the pre-positioning of MERs.

4. Case studies and discussion

This section presents the implementation and validation of the proposed approach through case studies on two modified distribution test systems, i.e., the 33-node system and the IEEE 123-node system.

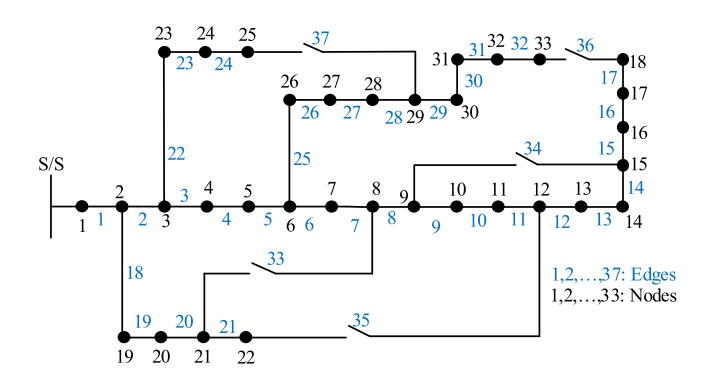


Fig. 5. 33-node distribution test system.

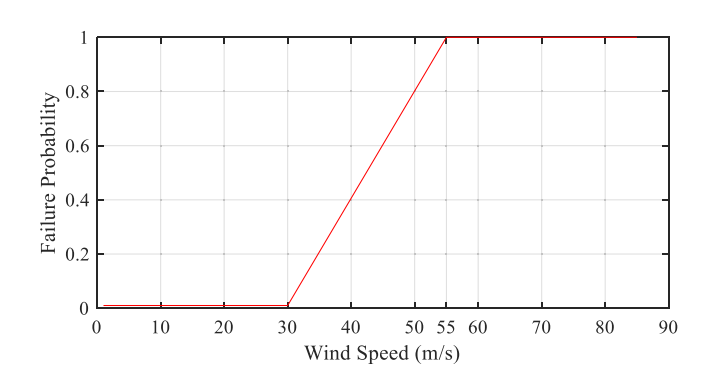


Fig. 6. Wind fragility curve for distribution lines.

4.1. Case study I: 33-node system

The 33-node distribution test system is a radial distribution system with 33 nodes, 32 branches, and 5 tie-lines (37 branches) [24]. All branches (including tie-lines) are numbered from 1 to 37 as shown in Fig. 5. The system's overall load is 3.71 MW. The locations and amounts of critical loads considered for the 33-node system are shown in Table A.10 of Appendix. The road network data considered for the 33-node system are shown in Table A.12 of Appendix.

For the implementation of the proposed approach, multiple line outage scenarios are generated by considering a high wind speed event as an example of a weather-related extreme event. The critical wind speed of 30 m/s and the collapse speed of 55 m/s are assumed for the fragility model (8) under consideration [18]. The failure probability of 0.01 is considered at normal weather conditions. The wind fragility curve for distribution lines adopted in the work is as shown in Fig. 6. In this article, 10,000 random

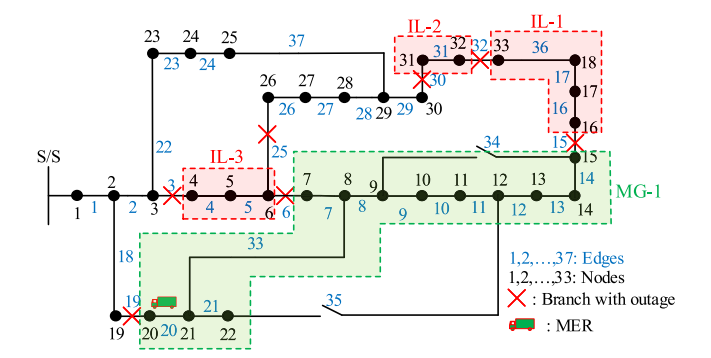


Fig. 7. An outage case for 33-node distribution system.

Table 1Comparison of scenario reduction for the 33-node system.

Index/Method	k-means	k-medians	Fuzzy k-means
SL index	0.0257	0.0119	0.0292
DB index	2.869	3.116	2.833
CH index	19.507	16.947	20.211

outage scenarios are generated and a fuzzy k-means method is used to reduce the generated scenarios into 200 reduced outage scenarios for wind speed of 38 m/s. The fuzzy k-means method outputs 200 reduced line outage scenarios along with their probabilities. The effectiveness of the fuzzy k-means method is compared with other clustering methods such as k-means and k-medians methods. Three indices, i.e., Silhouette (SL) index, Davies–Bouldin (DB) index, and Calinski–Harabasz (CH) index are used to compare the fuzzy k-means method with other clustering methods.

The SL index, which has values ranging from 1 to +1, is a measurement of how close a data point is with respect to its cluster in comparison to other clusters, as described in Section 3. A high number denotes that the data point is strongly matched with respect to its own cluster and weakly matched to nearby clusters. Similarly, the DB index makes use of the inherent characteristics and attributes of the dataset to validate the quality of the clustering and a lower value indicates a more effective clustering. The third index utilized in this article, the CH index, measures the degree of dispersion across clusters and a higher value for the CH index denotes more effective clustering. Table 1 shows the values of the indices for all three clustering methods. The comparison result shows that the fuzzy k-means is better than other methods (i.e., k-means and k-medians) in terms of all three indices.

For each reduced line outage scenario, the distribution network reconfiguration is performed using tie-switches present in the network and spanning forest is formed by deploying MER of capacity 1200 kW at a location (node). Fig. 7 shows the case for a reduced scenario where outages of lines 3, 6, 15, 19, 25, 30, and 32 occur. In this scenario, the distribution network is reconfigured by closing tie-switches 33, 36, and 37 using KSFSA. The tie-switches 34 and 35 are not closed to maintain radial configuration. When the MER is deployed at node 20, a microgrid (MG-1) and three isolates (IL-1, IL-2, and IL-3) are formed. These isolates are devoid of power supply. The total critical loads of IL-1, IL-2, and IL-3 are, respectively, 75 kW, 0 kW, and 150 kW. Therefore, when the MER is deployed at node 20, the total critical load curtailment for this reduced scenario is 225 kW. This process is repeated for all locations (nodes) and all reduced scenarios. The expected load curtailment (ELC) corresponding to each location then is determined based on load curtailment and probability of each reduced scenario.

Table 2Characteristic functions of possible coalitions for the 33-node system.

Coalitions	Expected critical load recovery (kW)
_	
7	102.6
8	103.5
9	108.0
21	103.5
7, 8	206.1
7, 9	210.7
7, 21	206.1
8, 9	205.0
8, 21	200.5
9, 21	205.0
7, 8, 9	296.7
7, 8, 21	290.3
7, 9, 21	296.7
8, 9, 21	280.9
7, 8, 9, 21	345.8

Table 3
Shapley values and sizes of MERs at candidate locations for 33-node system.

1 3			•
Locations (nodes)	Shapley values	MER sizes (proposed approach)	MER sizes (EDB approach)
7	96.25	320 kW	300 kW
8	88.65	290 kW	300 kW
9	92.87	300 kW	300 kW
21	88.65	290 kW	300 kW

MERs are assumed to be initially located at the substation node. The optimal path and distance of each node from the substation node is computed using DSPA. If only ELC is considered as the criterion for selecting candidate MER location, nodes 8, 9, 15, and 21 are obtained as candidate MER locations. Similarly, if only distance from the substation is considered as the criterion for selecting candidate MER location, nodes 2, 3, 4, and 19 are obtained as candidate MER locations since these nodes are closest to the substation. However, this work uses MER deployment cost based on both ELC and distance from the substation, which is computed using (19). The values of weighting coefficients β_1 and β_2 are taken as 0.9 and 0.1, respectively. The four locations (nodes 7, 8, 9, and 21) with least MER deployment costs are selected as candidate MER locations.

To compute the size of each MER, the four candidate MER locations are treated as players of the coalitional game. The characteristic function (here, the expected critical load recovery) is calculated for each set of possible coalitions. The expected critical load recovery (ECLR) is calculated by taking the difference of ELCs before and after MER placement. Before MER placement, the ELC of the system is 476.93 kW. The ECLR (or characteristic functions) for all sets of possible coalitions are shown in Table 2. We can see from the table that the ECLR for the coalition of locations 7 and 8 is equal to the sum of ECLRs of individual locations. However, the ECLR for the coalition of locations 8 and 9 is less than the sum of ECLRs of individual locations. This indicates that some coalitions are worthier than others and this property is utilized to compute Shapley values of individual candidate MER locations. The Shapley values and sizes of MER of each candidate location are shown in Table 3.

4.2. Case study II: IEEE 123-node system

Fig. 8 shows the modified IEEE 123-node distribution test system, which consists 123 nodes and 126 branches. Out of 126 branches, two of them (94–54 and 151–300) are equipped with tie-switches. All branches and loads are assumed to be balanced. The locations and amounts of critical loads considered for the

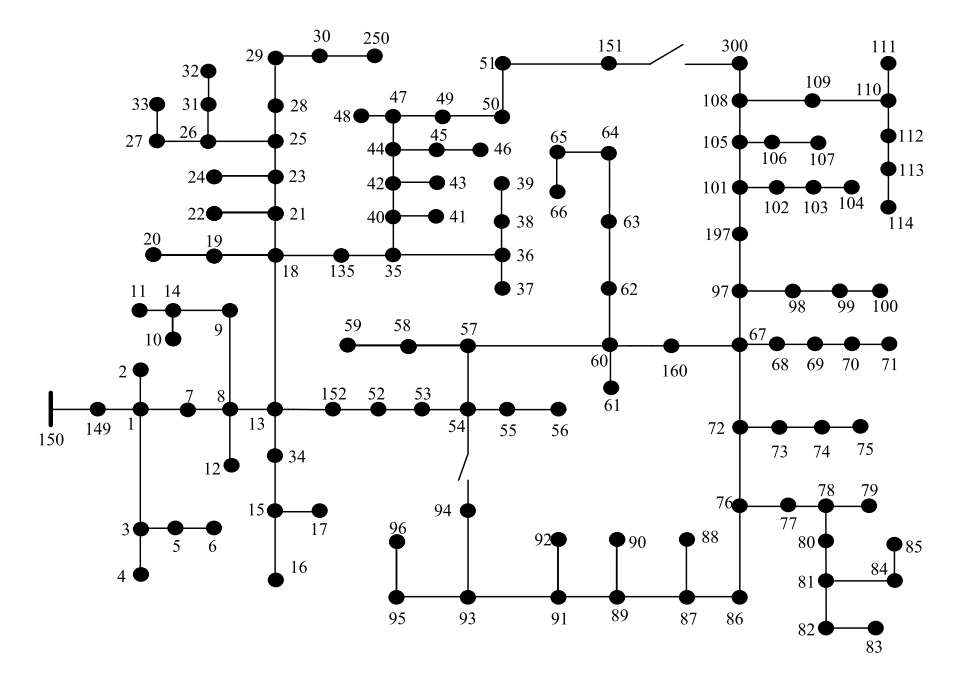


Fig. 8. IEEE 123-node distribution system.

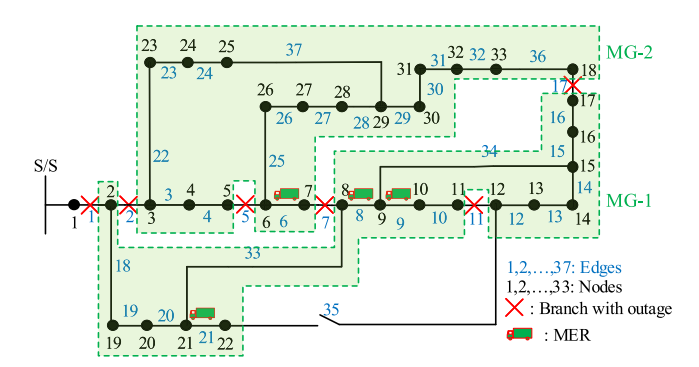


Fig. 9. Simulation of an outage scenario in case of 33-node system.

system are shown in Table A.11 of Appendix. The road network data for the system is shown in Table A.13 of Appendix.

Similar to the previous case study, 10,000 random outage scenarios are generated for this case and the fuzzy k-means method is used to get 200 reduced scenarios along with their probabilities. Table 4 shows the comparison of the fuzzy k-means method with other scenario reduction methods using three different indices. The comparison result shows that the fuzzy k-means is better than other methods for scenario reduction. For each reduced line outage scenario, the distribution network reconfiguration is performed using tie-switches and spanning forest is formed by deploying MER of capacity 1200 kW at each node. The ELC of each location is obtained by repeating the process for all reduced scenarios.

Similar to the previous case study, DSPA is used to calculate the optimal path and distance of each node from the substation node. If only ELC is considered as the criterion for selecting candidate MER locations, the candidate MER locations would be 66, 77, 86, 97, and 197. If only optimal distance is considered as the criterion for selecting candidate MER locations, the candidate MER locations would be 1, 2, 3, 7, and 149. However, the MER deployment cost function based on both ELC and optimal distance, with weighting coefficients of 0.9 and 0.1, respectively, has been considered in this work. As a result, the five locations (nodes 54,

Table 4Comparison of scenario reduction for the 123-node system.

Index/Method		k-means	k-medians	Fuzzy k-means
	SL index	-0.006	-0.001	0.010
	DB index	4.523	4.919	4.415
	CH index	5.851	5.262	6.597

Table 5Shapley values and sizes of MERs at candidate locations for the 123-node system.

Locations (nodes)	Shapley values	MER sizes (proposed approach)	MER sizes (EDB approach)
54	23.97	230 kW	240 kW
57	24.33	240 kW	240 kW
91	25.96	250 kW	240 kW
93	24.48	240 kW	240 kW
94	23.97	240 kW	240 kW

57, 91, 93, and 94) with least MER deployment cost functions are selected as the candidate MER locations.

Similar to the previous case study, a coalitional game is formulated and the expected critical load recovery is used as characteristic function for the game. Based on the characteristic functions of all possible sets of coalitions, Shapley values and CDF of candidate MER locations are determined. Finally, MER sizes are determined using total MER capacity and CDF of each candidate MER location. Table 5 shows Shapley values and sizes of MERs at each candidate location for the 123-node system.

4.3. Comparison

For both case studies, sizes of MERs obtained using the proposed approach are compared with an equal distribution-based (EDB) approach, where the total MER capacity is equally distributed at all candidate locations. Fig. 9 shows the case of the 33-node system for the outage of lines 1, 2, 5, 7, 11, and 17. After the implementation of KSFSA, all tie-switches are closed except tie-switch 35. For this scenario, MERs are placed at the candidate locations calculated based on least MER deployment cost functions. Two microgrids (MG-1 and MG-2) as shown in Fig. 9 are formed as a result of reconfiguration. MER sizes are, then,

Table 6Comparison of critical load curtailments and expected critical load curtailments.

Approaches/ Test Systems	33-node system scenario in Fig. 9	123-node system scenario in Fig. 10	33-node system (all reduced scenarios)	123-node system (all reduced scenarios)	
EBD Proposed	470 kW 460 kW	75 kW 65 kW	131.1345 kW 130.6315 kW	87.936 kW 87.887 kW	

Table 7Comparison of the 33-node system test cases based on ref. [25] with and without pre-positioning.

Cases	Without pre-position	ing	With Pre-positioning		
	Max distance (ft)	Max time (s)	Max distance (ft)	Max time (s)	
Test Case-I	3450	115	3200	106.667	
Test Case-II	3450	115	3200	106.667	

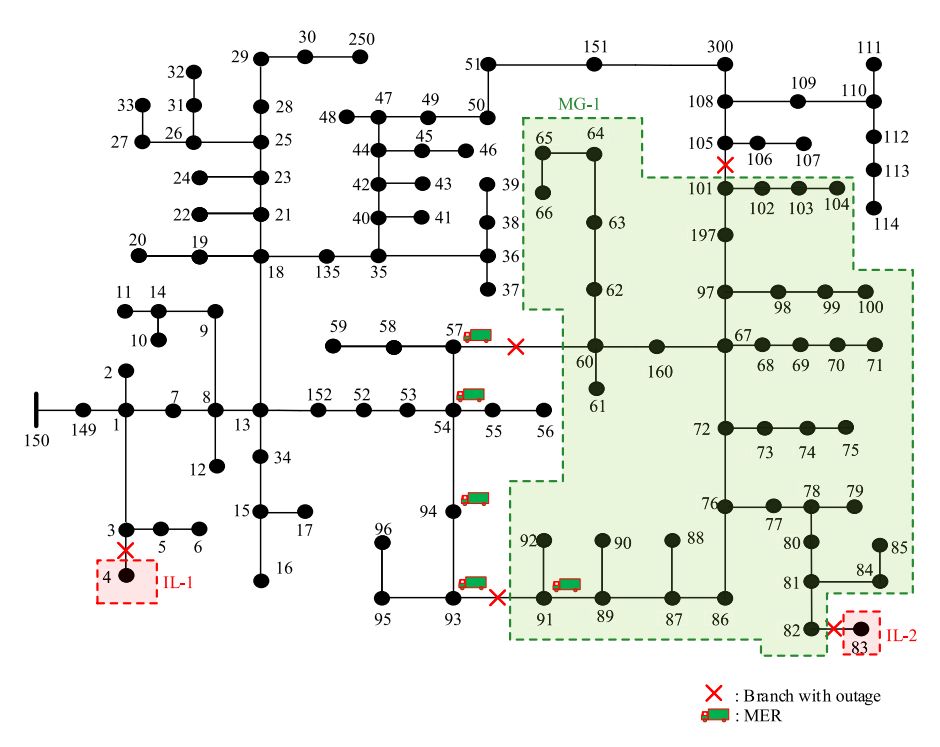


Fig. 10. Simulation of an outage scenario in case of the 123-node system.

chosen using both the proposed approach and EDB approach. When MER sizes are chosen using EDB approach, the amounts of curtailed critical loads in MG-1 and MG-2 are, respectively, 0 kW and 470 kW. This results in total critical load curtailment of 470 kW. However, when MER sizes are chosen using the proposed approach, the amounts of critical loads in MG-1 and MG-2 are, respectively, 0 kW and 460 kW, the total critical load curtailment amounting 460 kW. Therefore, the total critical load curtailment is reduced when MER sizes are determined based on the proposed approach.

Fig. 10 shows the case of the 123-node system for the outage of lines 3-4, 57-60, 82-83, 91-93, and 101-105. Both tieswitches 94-54 and 151-300 are closed after the implementation of KSFSA. When MERs are placed at locations 54, 57, 91, 93, and 94, a microgrid MG-1 and two isolates (IL-1 and IL-2) are formed as shown in Fig. 10 as a result of reconfiguration. Both of the isolates IL-1 and IL-2 do not have critical loads. When MER sizes are chosen using the EDB approach, the amount of curtailed critical load in MG-1 is 75 kW. However, when MER sizes are chosen using the proposed approach, the amount of curtailed critical load in MG-1 is reduced to 65 kW.

Figs. 9 and 10 show the cases for a particular line outage scenario. If the process is repeated for all reduced line outage

scenarios, the expected load curtailments are obtained for both approaches.

Table 6 shows the values of expected load curtailments for both approaches. The comparison result shows that the expected load curtailments are reduced with the proposed approach for both case studies.

4.4. Resilience evaluation based on recovery time

Resilience evaluation criteria are needed in order to analyze and assess resilience enhancement strategies. In the literature, a number of resilience evaluation and assessment criteria have been put forth, and some of these have been applied to the evaluation and assessment of power system resilience. Service interruption, outage duration, restoration cost, and preventive cost have all been utilized to assess power system resilience [26]. Additionally, due to the absence of widely accepted resilience metrics and evaluation criteria, resilience has been assessed using a number of stochastic and deterministic criteria, including load curtailment, load restoration, outage duration, and rate of recovery [27]. In the previous sub-sections, the enhancement of distribution system resilience was evaluated using the amount of

curtailed critical loads. This sub-section presents the evaluation of distribution resilience based on recovery time.

Table 7 shows the comparison of two test cases from our previous work [25] with and without pre-positioning for the 33-node system in terms of maximum traveling distance and maximum traveling time. The table shows that the traveling distance and time are reduced as a result of pre-positioning. The traveling speed is assumed to be 30 ft/s in this analysis. The recovery time in case of the 33-node system is reduced by 8.33 s for both test cases. It can, therefore, be concluded from the results that the proposed approach can reduce the recovery time, thereby enhancing the system resilience.

4.5. Limitations and benefits of the proposed approach

The proposed coalitional game theory-based approach suffers from scalability challenges. In our recent work [28], we have shown that the computational time of the coalitional game theory-based approaches increases non-linearly as the number of players or the size of system is increased. However, the proposed graph theory and coalitional game theory-based pre-positioning of MERs is still viable because pre-positioning is generally performed on week-ahead basis based on the availability of weather forecasting and monitoring data. The consideration of marginal contribution of each MER location while distributing the total MER size makes the coalitional game theoretic techniques based on Shapley values still favorable for pre-positioning of MERs.

5. Conclusion and future work

This article has proposed an approach based on graph theory and coalitional game theory for pre-positioning of movable energy resources (MERs) to improve resilience of the power supply. Multiple line outage scenarios were generated, and the fuzzy k-means method was used to reduce the generated scenarios. The distribution network and the road network were modeled as graphs. The characteristic function of the coalitional game model was computed for each possible set of coalitions based on expected critical load recovery. The Shapley value, one of the solution concepts of coalitional game theory, was then used to determine capacity distribution factor of each candidate MER location.

The case study results showed that the proposed approach can effectively determine the pre-positioning locations and sizes of MERs with the least expected critical load curtailments. The individual sizes of MERs obtained using the proposed approach were compared with the equal distribution-based (EDB) approach in terms of total critical load curtailments. The comparison results

showed that the total critical loads curtailments were reduced when MER sizes were determined based on the proposed approach for both the 33-node and the IEEE 123-node test systems. Because of the use of the Shapley value, which takes into account the average marginal contribution of each location, the proposed approach's main benefit is a fair allocation of the overall MER size among different candidate locations. Moreover, reliability enhancement was evaluated using two different resilience evaluation indices: expected critical load curtailment and recovery time. It was concluded from each case study that the proposed approach could effectively lower the expected value of curtailed critical loads. The comparison of test cases with and without pre-positioning also showed that the maximum traveling distances (or maximum traveling durations) were reduced, thereby lowering the recovery time and enhancing system resilience.

One of the future research directions of the proposed work could be the consideration of the dynamics of different distribution system components and performing stability analysis before selecting the pre-positioning locations and individual sizes of MERs. Also, integration of case studies of cyber-attacks along with weather-related outages and the development of cyber-physical resilience framework could be a possible extension of this work.

CRediT authorship contribution statement

Mukesh Gautam: Conceptualization, Methodology, Data curation, Writing – original draft, Software, Investigation, Data curation, Validation, Formal analysis. **Mohammed Benidris:** Conceptualization, Methodology, Supervision, Validation, Writing – review & editing.

Declaration of competing interest

The authors declare that they have no known competing financial interests or personal relationships that could have appeared to influence the work reported in this paper.

Data availability

Relevant data are in the article.

Acknowledgments

This work was supported by the U.S. National Science Foundation (NSF) under Grant NSF 1847578.

Appendix. Line parameters, critical loads, and road networks data

See Tables A.8-A.13.

Table A.8Line Parameters Data for 33-node System.

From node	To node	Impedance (Ω)	From node	To node	Impedance (Ω)
1	2	0.0922+j0.0470	17	18	0.7320+j0.5740
2	3	0.4930+j0.2511	2	19	0.1640+j0.1565
3	4	0.3660+j0.1864	19	20	1.5042+j1.3554
4	5	0.3811+j0.1941	20	21	0.4095+j0.4784
5	6	0.8190+j0.7070	21	22	0.7089+j0.9373
6	7	0.1872+j0.6188	3	23	0.4512+j0.3083
7	8	0.7114+j0.2351	23	24	0.8980+j0.7091
8	9	1.0300+j0.7400	24	25	0.8960+j0.7011
9	10	1.0440+j0.7400	6	26	0.2030+j0.1034
10	11	0.1966+j0.0650	26	27	0.2842+0.1447
11	12	0.3744+j0.1238	27	28	1.0590+j0.9337
12	13	1.4680+j1.1550	28	29	0.8042+j0.7006
13	14	0.5416+j0.7129	29	30	0.5075+j0.2585
14	15	0.5910+j0.5260	30	31	0.9744+j0.9630
15	16	0.7463+j0.5150	31	32	0.3105+j0.3619
16	17	1.2890+j1.7210	32	33	0.3410+j0.5302

Table A.9Line parameters data for the modified IEEE 123-node system.

From node	To node	Length (ft)	R (Ω/1000 ft)	X (Ω/1000 ft)	From node	To node	Length (ft)	R (Ω/1000 ft)	X (Ω/1000
1	2	175	0.4576	1.078	60	61	550	1.5209	0.7521
1	3	250	0.4666	1.0482	60	62	250	0.4576	1.078
1	7	300	0.4615	1.0651	62	63	175	0.4666	1.0482
3	4	200	1.3292	1.3475	63	64	350	0.4615	1.0651
3	5	325	1.5209	0.7521	64	65	425	1.3292	1.3475
i	6	250	0.4576	1.078	65	66	325	1.5209	0.7521
•	8	200	0.4666	1.0482	67	68	200	0.4576	1.078
3	12	225	0.4615	1.0651	67	72	275	0.4666	1.0482
3	9	225	1.3292	1.3475	67	97	250	0.4615	1.0651
3	13	300	1.5209	0.7521	68	69	275	1.3292	1.3475
,)	14	425	0.4576	1.078	69	70	325	1.5209	0.7521
3	34	150	0.4666	1.0482	70	71	275	0.4576	1.078
	18				70 72	73			
3		825	0.4615	1.0651			275	0.4666	1.0482
14	11	250	1.3292	1.3475	72	76	200	0.4615	1.0651
14	10	250	1.5209	0.7521	73	74	350	1.3292	1.3475
5	16	375	0.4576	1.078	74	75	400	1.5209	0.7521
5	17	350	0.4666	1.0482	76	77	400	0.4576	1.078
8	19	250	0.4615	1.0651	76	86	700	0.4666	1.0482
8	21	300	1.3292	1.3475	77	78	100	0.4615	1.0651
9	20	325	1.5209	0.7521	78	79	225	1.3292	1.3475
21	22	525	0.4576	1.078	78	80	475	1.5209	0.7521
1	23	250	0.4666	1.0482	80	81	475	0.4576	1.078
23	24	550	0.4615	1.0651	81	82	250	0.4666	1.0482
3	25	275	1.3292	1.3475	81	84	675	0.4615	1.0651
5	26	350	1.5209	0.7521	82	83	250	1.3292	1.3475
5	28	200	0.4576	1.078	84	85	475	1.5209	0.7521
6	27	275	0.4666	1.0482	86	87	450	0.4576	1.078
6	31	225	0.4615	1.0462	87	88	175	0.4666	1.0482
.0 !7	33	500	1.3292	1.3475	87	89	275	0.4615	1.0482
	29								
28		300	1.5209	0.7521	89	90	225	1.3292	1.3475
29	30	350	0.4576	1.078	89	91	225	1.5209	0.7521
80	250	200	0.4666	1.0482	91	92	300	0.4576	1.078
81	32	300	0.4615	1.0651	91	93	225	0.4666	1.0482
34	15	100	1.3292	1.3475	93	94	275	0.4615	1.0651
35	36	650	1.5209	0.7521	93	95	300	1.3292	1.3475
35	40	250	0.4576	1.078	95	96	200	1.5209	0.7521
36	37	300	0.4666	1.0482	97	98	275	0.4576	1.078
86	38	250	0.4615	1.0651	98	99	550	0.4666	1.0482
8	39	325	1.3292	1.3475	99	100	300	0.4615	1.0651
10	41	325	1.5209	0.7521	101	102	225	1.3292	1.3475
10	42	250	0.4576	1.078	101	105	275	1.5209	0.7521
12	43	500	0.4666	1.0482	102	103	325	0.4576	1.078
2	44	200	0.4615	1.0651	103	104	700	0.4666	1.0482
4	45	200	1.3292	1.3475	105	106	225	0.4615	1.0651
4	47	250	1.5209	0.7521	105	108	325	1.3292	1.3475
5	46	300	0.4576	1.078	106	108	575	1.5292	0.7521
:5 :7	46 48	150	0.4666	1.078	108	107	450	0.4576	1.078
· / ·7									
	49	250	0.4615	1.0651	108	300	1000	0.4666	1.0482
9	50	250	1.3292	1.3475	109	110	300	0.4615	1.0651
0	51	250	1.5209	0.7521	110	111	575	1.3292	1.3475
1	151	500	0.4576	1.078	110	112	125	1.5209	0.7521
2	53	200	0.4666	1.0482	112	113	525	0.4576	1.078
3	54	125	0.4615	1.0651	113	114	325	0.4666	1.0482
64	55	275	1.3292	1.3475	135	35	375	0.4615	1.0651
54	57	350	1.5209	0.7521	149	1	400	1.3292	1.3475
55	56	275	0.4576	1.078	152	52	400	1.5209	0.7521
.5 57	58	250	0.4666	1.0482	160	67	350	0.4576	1.078
57	60	750	0.4615	1.0651	197	101	250	0.4666	1.0482
58	59	250	1.3292	1.3475	137	101	230	0.4000	1.0-102

Table A.10Locations of critical loads for the 33-node system.

LUCATIONS OF	Locations of Critical loads for the 33-node system.						
Nodes	Critical loads (kW)	Nodes	Critical loads (kW)				
4	60	20	45				
5	30	21	45				
6	60	22	45				
7	200	23	45				
8	200	26	60				
9	60	27	60				
10	30	28	60				
11	25	29	60				
18	45	30	60				
19	45	33	30				

Table A.11 Locations of critical loads for the 123-node system.

Nodes	Critical loads (kW)	Nodes	Critical loads (kW)
1	40	66	75
6	40	75	40
11	40	79	40
17	20	85	40
24	40	87	40
30	40	94	40
37	40	98	40
43	40	100	40
50	40	109	40
52	40	113	40

Table A.12Road network data for 33-node system.

From node	To node	Distance (ft)	From node	To node	Distance (ft)
1	2	500	15	16	400
2	3	600	15	18	500
2	19	700	16	17	700
3	4	400	17	30	900
3	23	500	18	33	400
4	5	450	19	20	800
5	6	500	20	21	800
6	7	400	21	22	700
6	26	400	23	24	450
7	8	400	24	25	300
8	9	500	24	28	600
9	21	650	25	29	550
9	10	400	26	27	450
10	11	600	26	32	700
11	22	650	27	28	500
11	12	500	27	30	400
12	13	400	27	31	550
12	14	600	29	30	550
14	15	650	31	33	550
14	32	650	32	33	500

Table A.13Road network data for 123-node system.

From node	To node	Distance (ft)	From node	To node	Distance (ft)	From node	To node	Distance (ft
1	2	175	44	47	250	89	90	225
1	3	250	45	46	300	89	91	225
1	7	300	47	48	150	91	92	300
3	4	200	47	49	250	91	93	225
3	5	325	49	50	250	93	94	275
5	6	250	50	51	250	93	95	300
7	8	200	51	151	500	95	96	200
8	12	225	52	53	200	97	98	275
8	9	225	53	54	125	98	99	550
8	13	300	54	55	275	99	100	300
9	14	425	54	57	350	101	102	225
13	34	150	55	56	275	101	105	275
13	18	825	57	58	250	102	103	325
14	11	250	57	60	750	103	104	700
14	10	250	58	59	250	105	106	225
15	16	375	60	61	550	105	108	325
15	17	350	60	62	250	106	107	575
18	19	250	62	63	175	108	109	450
18	21	300	63	64	350	108	300	1000
19	20	325	64	65	425	109	110	300
21	22	525	65	66	325	110	111	575
21	23	250	67	68	200	110	112	125
23	24	550	67	72	275	112	113	525
23	25	275	67	97	250	113	114	325
25	26	350	68	69	275	135	35	375
25	28	200	69	70	325	149	1	400
26	27	275	70	71	275	152	52	400
26	31	225	72	73	275	160	67	350
27	33	500	72	76	200	197	101	250
28	29	300	73	74	350	150	149	250
29	30	350	74	75	400	13	152	250
30	250	200	76	77	400	18	135	300
31	32	300	76	86	700	60	160	300
34	15	100	77	78	100	97	197	300
35	36	650	78	79	225	94	54	400
35	40	250	78	80	475	151	300	500
36	37	300	80	81	475	2	10	400
36	38	250	81	82	250	20	27	800
38	39	325	81	84	675	32	29	500
40	41	325	82	83	250	51	250	800
40	42	250	84	85	475	4	16	900
42	43	500	86	87	450	82	86	600
42	44	200	87	88	175	37	62	500
44	45	200	87	89	275	100	114	600

References

- NOAA National Centers for Environmental Information (NCEI), U.S. billion-dollar weather and climate disasters, 2022.
- [2] M. Gautam, M. Benidris, Pre-positioning of movable energy resources for distribution system resilience enhancement, in: 2022 International Conference on Smart Energy Systems and Technologies, SEST, IEEE, 2022, pp. 1–6.
- [3] S. Lei, C. Chen, H. Zhou, Y. Hou, Routing and scheduling of mobile power sources for distribution system resilience enhancement, IEEE Trans. Smart Grid 10 (5) (2018) 5650–5662.
- [4] Z. Yang, P. Dehghanian, M. Nazemi, Enhancing seismic resilience of electric power distribution systems with mobile power sources, in: IEEE Industry Applications Society Annual Meeting, IEEE, 2019, pp. 1–7.
- [5] M. Nazemi, P. Dehghanian, X. Lu, C. Chen, Uncertainty-aware deployment of mobile energy storage systems for distribution grid resilience, IEEE Trans. Smart Grid 12 (4) (2021) 3200–3214.
- [6] J. Kim, Y. Dvorkin, Enhancing distribution resilience with mobile energy storage: A progressive hedging approach, in: 2018 IEEE Power & Energy Society General Meeting, PESGM, IEEE, 2018, pp. 1–5.
- [7] W. Sun, Y. Qiao, W. Liu, Economic scheduling of mobile energy storage in distribution networks based on equivalent reconfiguration method, Sustain. Energy, Grids and Netw. 32 (2022) 100879.
- [8] S.A. Sedgh, M. Doostizadeh, F. Aminifar, M. Shahidehpour, Resilient-enhancing critical load restoration using mobile power sources with incomplete information, Sustain. Energy, Grids and Netw. 26 (2021) 100418.
- [9] A. Gibbons, Algorithmic Graph Theory, Cambridge University Press, 1985.
- [10] A. Salles da Cunha, L. Simonetti, A. Lucena, Formulations and branchand-cut algorithm for the k-rooted mini-max spanning forest problem, in: International Conference on Network Optimization, Springer, 2011, pp. 43–50.
- [11] I.K. Ahani, M. Salari, S.M. Hosseini, M. Iori, Solution of minimum spanning forest problems with reliability constraints, Comput. Ind. Eng. 142 (2020) 106365
- [12] A. Katsigiannis, N. Anastopoulos, K. Nikas, N. Koziris, An approach to parallelize Kruskal's algorithm using helper threads, in: 2012 IEEE 26th International Parallel and Distributed Processing Symposium Workshops & PhD Forum, IEEE, 2012, pp. 1601–1610.
- [13] T.H. Cormen, C.E. Leiserson, R.L. Rivest, C. Stein, Introduction to algorithms, MIT Press, 2022.
- [14] M. Gautam, N. Bhusal, J. Thapa, M. Benidris, A cooperative game theory-based approach to formulation of distributed slack buses, Sustainable Energy, Grids and Netw. 32 (2022) 100890.

- [15] L.S. Shapley, M. Shubik, Competitive outcomes in the cores of market games, Internat. J. Game Theory 4 (4) (1975) 229–237.
- [16] I. Curiel, Cooperative Game Theory and Applications: Cooperative Games Arising from Combinatorial Optimization Problems, vol. 16, Springer Science & Business Media, 2013.
- [17] N. Bhusal, M. Gautam, M. Abdelmalak, M. Benidris, Modeling of natural disasters and extreme events for power system resilience enhancement and evaluation methods, in: 2020 International Conference on Probabilistic Methods Applied To Power Systems, PMAPS, IEEE, 2020, pp. 1–6.
- [18] M. Panteli, C. Pickering, S. Wilkinson, R. Dawson, P. Mancarella, Power system resilience to extreme weather: fragility modeling, probabilistic impact assessment, and adaptation measures, IEEE Trans. Power Syst. 32 (5) (2016) 3747–3757.
- [19] V.S. Rao, D.S. Vidyavathi, Comparative investigations and performance analysis of FCM and mfpcm algorithms on iris data, Indian J. Comput. Sci. Eng. 1 (2) (2010) 145–151.
- [20] X. Wang, Y. Xu, An improved index for clustering validation based on Silhouette index and Calinski-Harabasz index, in: IOP Conference Series: Materials Science and Engineering, 569, (5) IOP Publishing, 2019, 052024.
- [21] D.L. Davies, D.W. Bouldin, A cluster separation measure, IEEE Trans. Pattern Anal. Mach. Intell. (2) (1979) 224–227.
- [22] J. Ortiz-Bejar, M.R.A. Paternina, A. Zamora-Mendez, L. Lugnani, E. Tellez, Power system coherency assessment by the affinity propagation algorithm and distance correlation, Sustain. Energy, Grids and Netw. 30 (2022) 100658.
- [23] M. Gautam, E. Hotchkiss, M. Benidris, Determination of optimal size and number of movable energy resources for distribution system resilience enhancement, in: CIGRE Grid of the Future (GOTF) Symposium, CIGRE, 2022, pp. 1–6.
- [24] M.E. Baran, F.F. Wu, Network reconfiguration in distribution systems for loss reduction and load balancing, IEEE Power Eng. Rev. 9 (4) (1989) 101–102.
- [25] M. Gautam, N. Bhusal, M. Benidris, A deep reinforcement learning-based approach to post-disaster routing of movable energy resources, in: 2022 IEEE Industry Applications Society Annual Meeting, IAS, IEEE, 2022, pp. 1–6
- [26] H.H. Willis, K. Loa, et al., Measuring the resilience of energy distribution systems, RAND Corporation, Santa Monica, CA, USA, 2015, p. 38.
- [27] N. Bhusal, M. Abdelmalak, M. Kamruzzaman, M. Benidris, Power system resilience: Current practices, challenges, and future directions, IEEE Access 8 (2020) 18064–18086.
- [28] M. Gautam, M. Benidris, Coalitional game theory in power systems: Applications, challenges, and future directions, in: 2023 IEEE Texas Power and Energy Conference, TPEC, IEEE, 2023, pp. 1–5.